Keywords
Arc discharge in liquid, CuO nanoparticles, Ag/Zn doping, MB ,Photocatalytic degradation, Antibacterial activity

Authors
Mustafa H.hashim[1] ,
1 (Department of Physics, College of Education, University of Al-Qadisiyah, Iraq)
Mail: edu-phy.post2@qu.edu.iq
Orcid Id: 0009-0008-8562-239X

Abdulhussain A.khadayeir[2]
2 (Department of Physics, College of Education, University of Al-Qadisiyah ,Iraq (
Mail: abdulhussain.khadyair@qu.edu.iq
Orcid Id: 0000-0002-2945-5629

European Journal of Prosthodontics and Restorative Dentistry (2026) 34,7(s) 1188–1197

# CuO Pure and Doped Nanoparticle Synthesis and Characterization by Liquid Plasma and Applications for Methylene Blue Degradation and Antibacterial Bioactivity

**Abstract**
The production of pure copper oxide and doped (Ag, ZnO) nanoparticles by arc discharge. (5A) in distilled water, a simple, single-step, environmentally friendly technique which does not involve toxic reducing agents, electrolytes, and post-synthesis thermal treatment, has been reported in this paper. The creation was validated by X-ray diffraction analysis of the monoclinic CuO (tenorite) phase. At the same time, the Ag-doped samples showed an additional face-centered cubic metallic silver phase, and the ZnO-doped samples showed a hexagonal wurtzite ZnO phase with a monoclinic CuO phase. No impurity phases were detected. Scanning electron microscopy showed that the nanostructures had shapes ranging from spherical to irregular, porous, and aggregated. Surface roughness increased with doping. The nanoparticles were tested for under UV light, photocatalytic activity breaks down the dye methylene blue(MB). Pure CuO showed a degradation efficiency of ~92–93% within 135 min. In contrast, Ag-doped CuO achieved degradation of >98% in 90 min, and ZnO-doped CuO achieved degradation of >95% in 60 min, highlighting the role of doping in improving the separation of charge and the formation of reactive oxygen species. The antibacterial and antibiofilm activity of the nanoparticles was further assessed in comparison to clinical isolates of Klebsiella pneumoniae. It demonstrated concentration-dependent inhibition of bacterial adhesion and biofilm formation, with CuO: Ag showing the strongest antibacterial effect and CuO: ZnO showing the highest anti-biofilm activity. The results show that arc discharge in liquid is a rapid, economical, and additive-free method for manufacturing of pure and doped copper oxide(CuO) nanoparticles that can be applied for water purification and antibacterial applications.

Received:05-06-2026
Revised:17-07-2026
Accepted:03-08-2026
Doi:10.1922/ejprd.v34i7s.1769

## INTRODUCTION

Juvenile idiopathic arthritis remains the most prevalent chronic rheumatic disease of childhood and is an essentially

Nanomaterials are materials that possess at least one dimension in the nanometre scale, usually less than 100 nm [1]. Nanomaterials have garnered significant interest due to their distinctive characteristics. with their bulk counterparts. Small size, large surface area, and unusual chemical and physical properties make them suitable for a wide range of applications. [2-4]. Among them, metal and metal oxide nanoparticles (NPs) have attracted particular interest due to their enhanced properties, enabling diverse applications across multiple fields [5,6]. In particular, copper oxide nanoparticles have shown great potential in medicine [7–9], agricultur [10–12], and semiconductors [13,14].The shape and structure of copper oxide nanomaterials formed during synthesis are key factors determining their properties and applications. The most commonly reported morphologies are nanowires [13,14], nano-flowers [15,16], and spherical nanoparticles [17] , which were used as very effective photocatalysts [18], gas sensors [19,20] and supercapacitor electrodes [21]. Copper oxide by itself is less toxic [22], but its synthesis typically involves otherwise highly toxic compounds, particularly in efficient chemical processes that use reducing agents [23]. Sol-gel technique [26], laser ablation [25], and chemical vapour deposition [24] and biological synthesis as the other conventional direct or indirect approaches have limitations in terms of cost, complexity and/or adverse environmental impact. Doping silver (Ag) into CuO has improved the functional properties of materials, including charge transfer, electrical conductivity and photocatalytic activity. Ag nanoparticles deposited on the CuO surface generate LSPR to enhance light absorption and trigger ROS generation for pollutant degradation. Thus, Ag-doped CuO has the potential for use in water purification and air quality management,anti-microbial coatings and solar driven catalysis [28]. Typically, the photocatalytic activity of pure CuO nanoparticles are restricted because of fast recombine and loss process in photoinduced electron–hole pair pairs. In order to solve this problem, CuO was compounded with other metal oxides (most commonly Zn) and combined to make cupric oxide-zinc oxide nanocomposites (CuO:ZnO). It contributes to the heterojunction, which is expected to improve charge separation and reduce electron–hole ($e^-/h^+$) recombination thus increasing performance in these materials [29]. Several other discharge-based methods can also be used to create copper nanoparticles. In (2021), Efimov et al, synthesised copper oxide nanoparticles by dry aerosol jet printing using a spark discharge technique.[30].In (2020) Glad et al, used spark discharge in water, and they controlled the size of the copper and copper oxide particles produced by the addition of tiny concentrations of HCl to control the electrical conductivity of the solution. [31].When comparing these techniques, energy efficiency should be considered, Spark discharge usually requires a higher voltage than arc discharge.In addition, the presence of electrolytes may stabilise the liquid medium's arc discharge, their use introduces additional side electrochemical reactions that complicate the process [32].The proposed arc discharge technique in deionized water, therefore, offers an energy-efficient, simple, eco-friendly, and rapid alternative for producing copper oxide nanoparticles. More recently, Fomina et al. (2025) examined Bioactive properties of Janus-like CuO:Ag NPs against clinical isolates of Klebsiella pneumoniae.They reported that the antibiofilm activity of these particles at subinhibitory doses was 2- to 10-fold greater than that of a mechanical combination of separate CuO and Ag particles. [33].It has also been reported that the liquid plasma interaction produces reducing agents that speed up the decrease in metal ions [34], and that low currents of a few amperes are advantageous during arc discharge in liquid, since higher currents generate high temperatures that can cause excessive electrode erosion [35,36]. Variations during the arc discharge can affect the primary reactions of ionization and water splitting in the liquid phase, thereby influencing the composition and structure of the synthesised particles.[37,38]. Recent studies have also investigated the direct synthesis of particles from electrodes in water without electrolytes or reducing agents [39].Importantly, discharge in an oxygen-containing liquid medium leads to oxidation of metal particles without post-synthesis thermal annealing, potentially producing monodisperse oxide nanoparticles not only of copper but also of other metals. In this study, arc discharge plasma technology generated between copper, (Cu-Ag), and (Cu-Zn) electrode pairs immersed in water was used as a simple, environmentally friendly method to produce pure and doped copper oxide nanoparticles, with water serving as both the oxygen source and the dielectric medium. This approach does not employ toxic gases and chemical additions like electrolytes and reducing agents. A 5-amp arc discharge in water was the key controlling factor in the nanoparticle synthesis process. Unlike previous methods, this method requires neither additives nor post-heat treatment and has enabled the direct production of a variety of doped and pure copper oxide nanoparticles from electrodes in a single, easy process. The direct arc discharge technique described here allows for the synthesis of pure and doped copper oxide nanoparticles, which were tested for methylene blue (MB) dye degradation in the aqueous phase as well as for their antibacterial activity against Klebsiella pneumoniae.

## 2. MATERIALS & METHODS

### 2.1 Nanoparticles Synthesis:

In deionized water, arc discharge was used to create pure copper oxide particles doped with soluble silver and zinc. . Arc Discharge (schematic): Fig. 1 illustrates the arc discharge principle.Which is composed of a DC power supply and two electrodes with a distance of several mm between them, where the positions of the electrodes alternate between copper-silver and copper-zinc. We placed the electrodes within a glass vessel containing deionized water. The current in the plasma arc was 5 amperes. A dark precipitate was formed from the generated plasma. After that, the mixture was allowed to sit at room temperature for six hours to promote the development and expansion of nanoparticles. After that, the water was harvested and centrifuged to separate nanoparticles. The insoluble phase was centrifuged and thoroughly washed multiple times removing leftover ions or the unreacted feedstock with ethanol and distilled water. The nanoparticles (dark precipitate) were transferred to a glass slide and heated in the oven at 80 °C, then annealed at 450 °C for 2 hours in an electric furnace to complete the crystallization and phase formation. Finally, pure CuO, CuO: Ag, and CuO : ZnO powder nanoparticles were produced. Structural properties of nanoparticles were studied by X-ray diffraction and scanning electron microscopy.

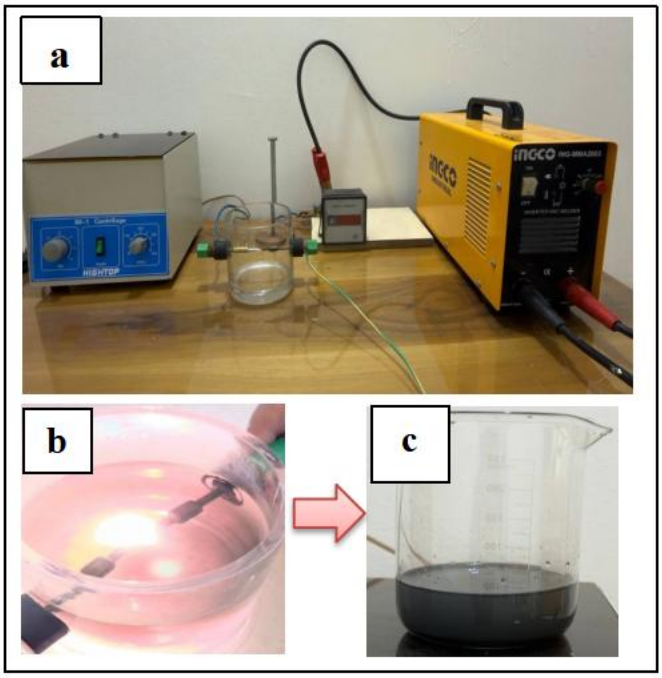


**Fig 1. (a) Experimental setup diagram (b) Arc discharge in water (c) Copper oxide particle solution obtained at a 5 A current**.

2.2 Photocatalytic:

The capacity of copper oxide nanoparticles to remove colours from polluted water by photocatalysis was investigated.With methylene blue (C16H18ClN3S·H2O; molecular weight: 319.86 g/mol) as a model dye. This dye was chosen to evaluate the photocatalytic efficiency. The photocatalytic reaction was carried out in a homemade reactor for photocatalysis. The reactor consisted of an ultraviolet lamp as the light source, a high-pressure pump (300 W, 220-240 V, manufactured by Philips Netherlands), a 200 mL Pyrex glass beaker, a magnetic actuator, a clamp, and a fan. The UV lamp was positioned 20 cm above the beaker, while the magnetic actuator was positioned below it. A magnetic motor was used to rotate the dye (at 800 rpm) with the photocatalyst. A basic methylene blue solution of 10 ppm was produced simply mixing 1000 millilitres of distilled water with one gram of methylene blue. The concentration of methylene blue (MB) was determined using a UV-Vis spectrophotometer by measuring the maximum absorption at 664 nm. Subsequently, 20 mg of particles (pure and impure copper oxide prepared using liquid plasma) were added to the flask containing the 10 ppm methylene blue solution. For 15 minutes, the mixture was agitated at room temperature. UV absorption equilibrium was achieved by incubating the catalyst-loaded dye solution in the dark for 30 minutes before UV exposure. After that, the solution was revealed to UV light, and 5 mL of the sample was withdrawn every 15 minutes using a microtube. The resulting nanoparticle powder was separated by centrifugation (in a Hettich Mikro 22R centrifuge) at 4000 rpm for 15 minutes. This lysed solution was then used to measure absorbance. Finally, The samples were analyzed on a UV-Vis spectrometer (Agilent Technologies) at 664 nm.

2.3 Antibacterial Activity

Clinical isolates of Klebsiella pneumoniae were obtained from Al-Diwaniyah Teaching Hospital and sub-cultured on MacConkey/Nutrient agar (37°C, 18–24 h). A single colony was grown overnight in TSB (1% glucose, 37°C, 18–24 h), modified to 0.5 McFarland standard (approximately $1.5 \times 10^8$ CFU/mL), and diluted 1:100 prior to use. Nanoparticle suspensions CuO, CuO:Ag, and CuO:ZnO were prepared in deionized water at four concentrations (125, 250, 500, and 1000 mg/mL) by vortexing and ultrasonic (15–30 min). Biofilm formation was evaluated using the microtiter plate assay. Bacterial suspension (100 µL) and nanoparticle suspension (100 µL) were added to 96-well plates in triplicate, with bacteria-only and medium-only wells as positive and negative controls, respectively. Plates underwent static incubation (37°C, 24 h), washed with PBS to remove non-adherent cells, and preserved with 100% methanol (15min). After 15 minutes of 0.1% crystal violet dyeing, the biofilms were cleaned with distilled water. The dye that was bonded was dissolved with 95% ethanol for 15 min, and biofilm inhibition was quantified by absorbance at 570 nm with an (ELISA) microplate reader.

## 3. RESULTS & DISCUSSION

### 3.1.1 X-ray diffraction analyses

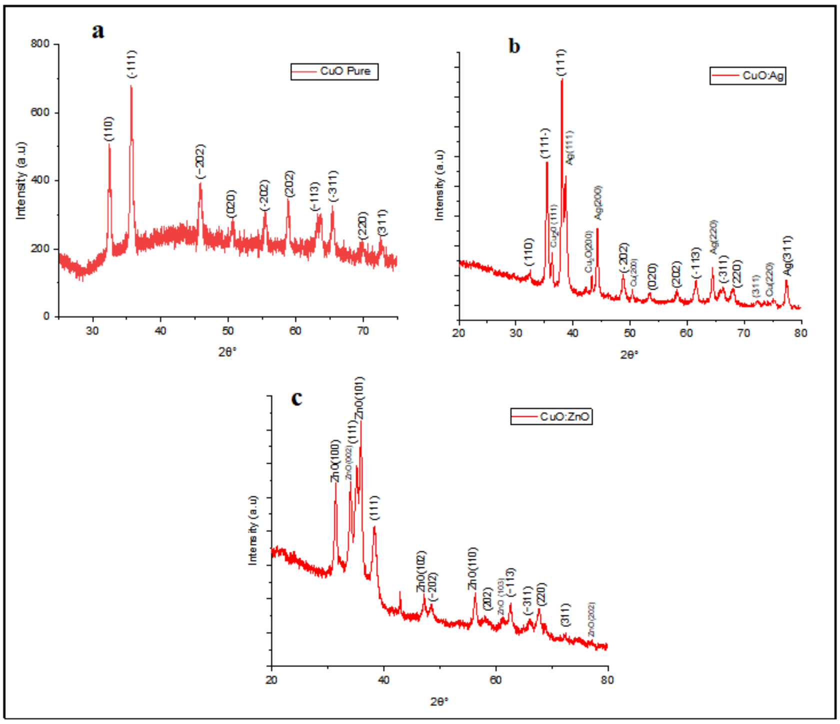


**Figure 2. X-ray pattern of diffraction of nanoparticle synthesis from (a) pure copper oxide, (b) silver-doped copper oxide, (c) zinc oxide-doped copper oxide using liquid plasma technology.**

X-ray diffraction was used to characterize the copper oxide nanoparticles. One of the most dependable and widely used techniques for figuring out the crystalline phase is X-ray diffraction, crystal size, and structural flaws in nanomaterials. The diffraction pattern measured for the current copper oxide sample in a 2θ range from 20° to 80° with Cu Kα radiation (λ = 1.5406 Å) clearly indicated the production of a highly crystalline copper oxide phase.The observed diffraction peaks .Figure (2a). The diffraction pattern showed peaks at 2θ angles of 32.4°, 35.6°, 45.8°, 50.5°, 55.4°, 58.9°, 62.2°, 65.5°, 69.0°, and 72.5° corresponding to the crystalline planes (110), (–111), (–202), (020), (–202), (202), (−113), (–311), (220), and (311), respectively, Those are features of the monoclinic phase of CuO. These findings are well in accord with standard reference data for CuO (JCPDS card 89-2531), which verifies that the synthesised material crystallises with a monoclinic structure. These findings are supported by similar diffraction patterns reported for CuO nanoparticles prepared by solution-based methods [40]. No more Cu2O-related peaks or metallic copper phase suggests that the obtained product is a pure CuO phase without secondary impurities. The crystallite size (D) results were calculated utilizing Debye-Scherrer equations given by:

$$D = (K\lambda) / (\beta \cos \theta)$$

where K - shape factor (K = 0.9), λ - wavelength of incident X-rays, β - full width at half height (FWHM) of the chosen diffraction peak (in radians), and θ is the Bragg diffraction angle [41]. Figure (2b). Shows the X-ray diffraction spectrum of the nanoparticles, in which Bragg reflections indicate peaks at 2θ = 32.74°, 35.77° and 38.95°, corresponding to planes (110), (002) and (111). Confirm that CuO nanoparticles are formed in a monoclinic structure (Renuga et al., 2020). [42]. Has indicated a cubic silver structure with angles 38.3°, 44.3°, 64.4° and 77.4°, which were related to levels (111), (200), (220) and (311), respectively, based on the JCPDS card number (04–0783). The major peaks at ~32.4°, 35.4°, 38.1°, 48.7°, 53.3°, 58.1°, 61.5°, 66.2°, 68.1°, and 72.4° correspond to levels (110), (−111), (111), (−202), (020), (202), (−113), (−311), (220), and (311), which are consistent with the monoclinic tenorite phase of CuO according to JCPDS card number (48-1548) [45]. The other peaks at ~38.1°, 44.3°, 64.4°, and 77.5° were attributed to metallic silver (Ag) with a cubic structure with a face center on (111), (200), (220), and (311) planes, respectively, corresponding to ICDD (04-0783) [31]. This indicates successful silver doping of copper oxide phases and the absence of other unwanted materials [46]. Because the CuO peak positions remained similar, the silver doping did not alter the fundamental crystal structure of CuO; instead, it led to the deposition of metallic silver either at the surface or at grain boundaries. The greater peak intensity and relative narrowness also indicate higher crystalline quality, meaning fewer crystal defects in the doped samples than in the undoped ones. As an electron sink, silver inhibits recombination between electrons and holes in the conduction band, which increases ROS production. This, in turn, benefits antibacterial activity, gas sensitivity, and optical properties. In particular, the presence of $Cu_2O$ and metallic copper phases shows that the preparation process allowed partial oxidation of copper, leaving some in its metallic form. The significant peaks at 2θ ≈ 36.4°, 42.3°, and 73.5° match the planes (111), (200), and (311) of the cubic $Cu_2O$ phase, in accordance with ICDD PDF card (78–2076) or ( 05–0667) [47]. The peaks at 50.3° and

74.9° correspond to metallic copper and correspond to the (200) and (220) planes, according to ICDD card 04-0836 [48]. The particles prepared by the plasma arc in deionized water contained Cu, $Cu_2O$, and CuO phases together, and the ratios of these phases depend on the discharge current conditions, indicating that oxidation during the plasma process may be partial and incomplete [49]. Figure 2c. Two different crystalline phases were formed, according to X-ray diffraction analysis, confirming the successful synthesis of the CuO/ZnO nanocomposite: Zinc oxide (ZnO) - hexagonal wurtzite phase.Peaks appeared at 31.3°, 34.0°, 35.85°, 56.2°, and 77.0°, corresponding to crystalline planes (100), (002), (101), (102), (110), and (202), respectively. These peaks are consistent with JCPDS card (36-1451), confirming the formation of the hexagonal wurtzite phase of zinc oxide. Monoclinic Copper Oxide (CuO) Phase. Peaks appeared at 35.14°, 38.37°, 48.54°, 58.19°, 62.5°, 67.6°, and 72.4°, corresponding to the levels (−111), (111), (−202), (202), (−113), (220), and (311), which are consistent with JCPDS card (48-1548) for the monoclinic CuO phase. The consistency of the peak positions with standard reference cards, along with the absence of additional peaks attributable to secondary phases or impurities, confirms effective fabrication of high crystalline purity of CuO:ZnO composite. The slight deviations observed in the positions of some peaks compared to the standard values are attributed to doping, crystal stress, or the small crystal size of the nanoparticles, phenomena common in nanomaterials prepared by various methods [50].

3.1.2 SEM analyses:

The scanning electron microscope (SEM) image of extremely crystalline CuO nanoparticles is shown in Fig.3. The SEM image clearly shows a coarse aggregate with spherical nano-homogeneities of CuO nanoparticles [51]. Figure 4 shows nanoparticles with spherical to irregular shapes and agglomerations, creating a permeable structure, lattice-structured formation as illustrated. The coarse textures and nanotexture are evidently discernible, showing equal distribution of particles. Ag doping has resulted in morphological changes and an increase in surface roughness, thereby improving the photocatalytic activity [28]. Figure 5 shows CuO nanoparticles doped with ZnO using scanning electron microscope images. The resulting particles are nanoscale in size and shape, and they aggregate, indicating The total segregation is not accomplished. The CuO:ZnO nanoparticles exhibit an overlapping sheet-like appearance[52].

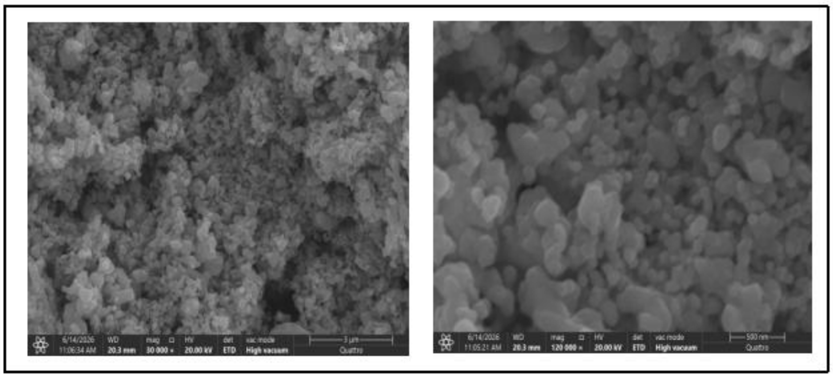

**Figure 3. Scanning electron micrographs of pure CuO nanoparticles synthesized using liquid plasma technology at different magnifications**.

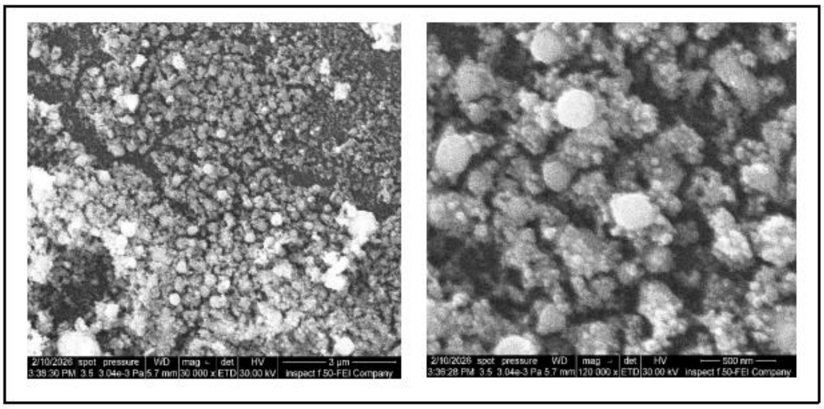

**Figure 4. Scanning electron micrographs of Ag-doped CuO nanoparticles fabricated using liquid plasma technology at different magnifications**.

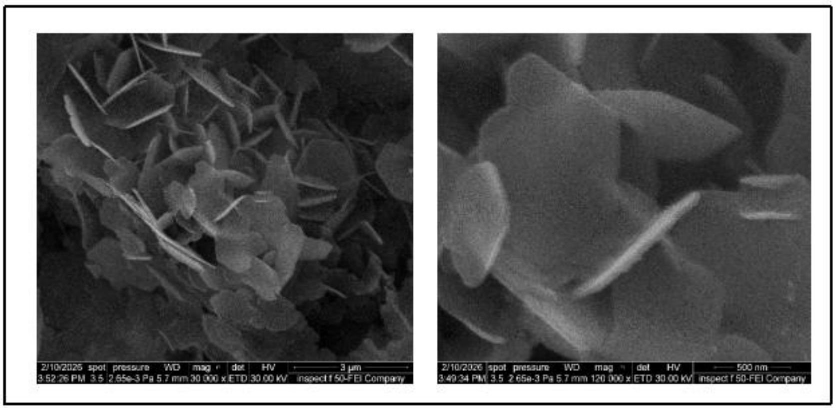


**Figure 5. Scanning electron micrographs of ZnO-doped CuO nanoparticles fabricated using liquid plasma technology at different magnifications**.

3.2 Photocatalytic analysis

The Figure(6a) shows a significant, gradual decrease in absorption peak of methylene blue dye at 664nm as the irradiation time increases from 15 to 135 minutes in the presence of pure CuO. This reflects the actual decomposition of the dye due to the formation of active radicals (•OH and •O2⁻) generated by the electron-hole pair ($e^-/h^+$) reaction resulting from CuO's absorption of light with water and dissolved oxygen. The decomposition efficiency reaches approximately 92–93% over 135 minutes. Comparing this result to the study by Khedr & Ali (2024) [53] . which used green-processed CuO and achieved a degradation efficiency of 95.34% within 120 minutes, yielded similar results, although the time required was slightly longer. This indicates that pure CuO possesses very good photocatalytic activity. Figure (6b) shows the photolysis process using a silver-doped copper oxide (CuO:Ag) catalyst. A rapid decrease in absorption intensity at 664 nm is observed as the irradiation time increases from only 15 to 90 minutes.The final degradation efficiency within 90 minutes is over 98%, a remarkable improvement over pure copper oxide (CuO). This notable performance improvement is attributed to silver (Ag), which enhances visible-light harvesting and broadens charge separation, increasing the synthesis of reactive oxygen species (ROS) and accelerating dye deterioration. Comparing these results with a study by Zulfiqar et al. (2026), which directly compared chemically synthesized Ag-CuO samples with those produced using the greensynthesis method, the green synthesis sample achieved a degradation efficiency of 95% within 80 minutes, while the chemically synthesized sample achieved an efficiency of 82% in the same time period [28]. These results indicate the superiority of the results obtained in dye decomposition. Figure (6c) shows the photocatalytic decomposition process using a copper oxide catalyst doped with zinc oxide (CuO:ZnO) to decompose methylene blue (MB) dye under UV-Vis irradiation. Rapid decay of absorbance intensity at 664 nm was observed as the irradiation duration increased from only 15 to 60 minutes. The overall decomposition efficiency exceeded 95% within 60 minutes, an excellent result compared to pure copper oxide (CuO), indicating that these compounds exhibited superior catalytic activity under optimal photocatalytic conditions. The composites exhibit a synergistic effect, a good connection between CuO and ZnO, which increases the photocatalytic activity. This significant performance improvement is attributed to the role of ZnO, which enhances light absorption is enhanced, and charge separation is optimised. The results I obtained were better, reaching a decomposition rate of 95% within 60 minutes, while the results obtained by Paramasivam Shanmugam et al. (2023) reached a decomposition rate of 98.5% within 150 minutes [54].Although the current sample reached a slightly lower final decay rate, it achieved this in less than half the time (60 vs.150 minutes), which is consistent with a much higher decay rate. This demonstrates that the CuO:ZnO catalyst used in this study is more efficient than both pure copper and Ag-doped copper.

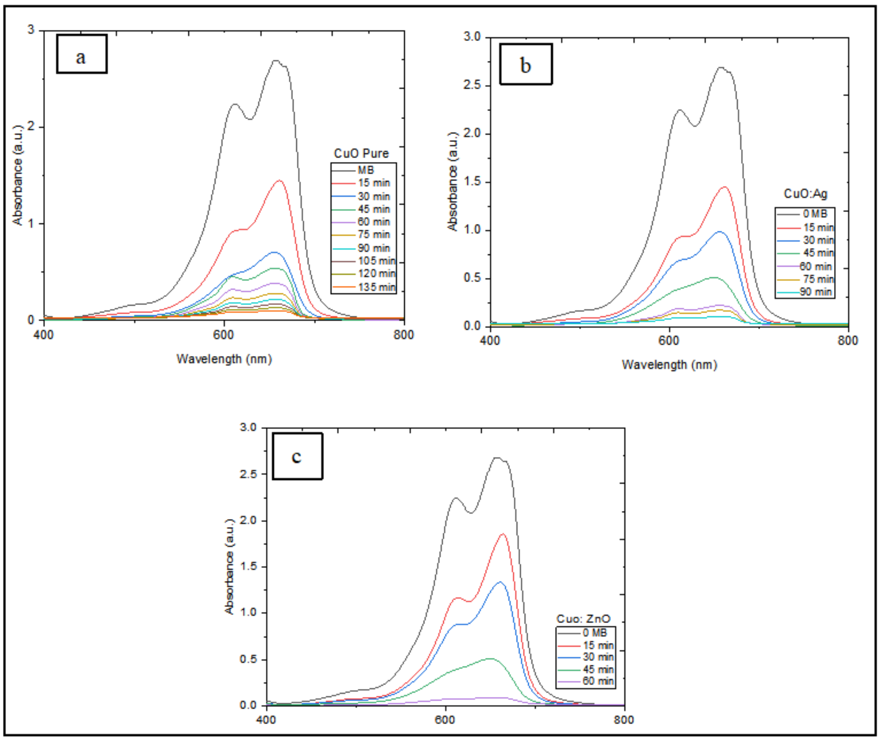


**Figure 6. Catalytic photolysis of methylene blue (MB) dye by using (a) CuO pure, (b) CuO:Ag ,(c) CuO:ZnO**

### 3.3 Antibacterial Activity analysis

Figure (7a) shows the results of bacterial adhesion. The graph measures the adhesion of Klebsiella pneumoniae bacteria (in cfu/ml) after exposure to increasing concentrations of three different kinds of nanoparticles: single CuO, CuO:Ag, and CuO:ZnO. The inhibition of adhesion by copper oxide (CuO) is as follows: Adhesion relies primarily on surface structures such as fimbriae and pili, which enable bacteria to attach to surfaces. CuO nanoparticles interfere with these structures by directly adhering to the cell wall and disrupting the bacteria's negative surface charge. This generates reactive oxygen species (ROS), which oxidize surface proteins involved in adhesion, thereby releasing $Cu^{2+}$ ions that interfere with cilia formation. CuO nanoparticles showed a gradual decrease in bacterial adhesion as the concentration increased from ~0.13 to ~0.072 cfu/ml (a decrease of ~64%). This result is consistent with studies confirming that CuO nanoparticles inhibit the initial adhesion of bacteria [55].While CuO:Ag particles showed the highest effectiveness in inhibiting bacterial adhesion among all groups, the value decreased from ~0.13 to ~0.052 at a concentration of 1000 mg/ml (a decrease of ~60%).When copper oxide is doped with silver, it creates a truly synergistic effect. The silver ions ($Ag^{+}$) inactivate respiratory enzymes and bind to thiol groups (-SH) in membrane proteins more efficiently than copper alone, which explains the greater decrease in CFU/ml values at high concentrations. Nanoparticles also modulate the gene expression of many important adhesins, thereby affecting the bacterial ability to adhere to and colonize surfaces [56].CuO:ZnO particles showed effectiveness in inhibiting bacterial adhesion, as the value decreased from ~0.11 to ~0.083 cfu/ml. When zinc oxide is added to copper oxide, zinc ions ($Zn^{+}$) are more soluble than copper ions, resulting in faster, more diffuse availability of the antibacterial ions. This explains the strong inhibition even at relatively low concentrations [57]. Bacterial adhesion is the first critical step in colonization and pathogenesis, this step may be disrupted by Ag and Cu nanoparticles due to the toxicity of these compounds.The results shown in Figure (7b) demonstrated a clear difference in the ability to inhibit biofilm formation between the tested treatments, with the control group maintaining the highest optical density reading (O.D $\approx 3.7\times10^{6}$) with relative consistency across all concentrations, reflecting normal, unhindered growth and formation of the biofilm in the absence of any antibacterial agent.In contrast, treating bacteria with copper oxide (CuO) nanoparticles and their compounds with silver (CuO:Ag) and zinc oxide (CuO:ZnO) resulted in a gradual and regular decrease in O.D values as the concentration increased from 125 to 1000 mg/ml, indicating an inverse relationship between the nanoparticle concentration and the mass of the biofilm formed, a dose-dependent inhibition pattern consistent with Ayman K. El-Sawaf et al.(2024) that used the same methodology based on measuring optical density and calculating the percentage of biofilm inhibition to evaluate the effectiveness of similar nanoparticle compounds against multidrug-resistant bacterial pathogens.While pure CuO particles were relatively less effective, they still exhibited concentration-dependent inhibition)[58].Shehabeldine et al.(2022) reported a 49–59% reduction at 0.5×MIC against K. oxytoca and E. coli, attributing this to the toxicity of copper ions ($Cu^{2+}$), their generation of ROS, and their reduction of EPS production[59]. The CuO:ZnO compound showed significantly higher activity than single copper oxide at all concentrations, in accordance with the findings of Moupiya Ghosh et al (2026), who showed significantly increased antimicrobial and anti-biofilm properties of the CuO-ZnO compound compared to the untreated base material against Escherichia coli and Staphylococcus aureus. This improvement is explained by the synergistic effect of combining zinc ions with copper [60].While CuO:Ag particles exhibited the strongest inhibitory effect among all tested treatments, yielding the lowest O.D. values at the highest concentration (1000 mg/ml), this aligns with a study by Saklani Taru et al,(2024). which found that the non-calcified form of CuO/Ag was the most potent antibacterial agent, with inhibition zones reaching up to 20 mm against Escherichia coli, Salmonella enterica with Staphylococcus aureus[61]. The advantage of silver ions is due to the better capacity to promote the production of reactive oxygen species (ROS) and to disrupt bacterial cell membrane permeability more effectively than pure copper.This mechanism is further supported by a study by Fatima Alhosani et al (2025) [62]. In some cases, such as zinc oxide nanoparticles, more effective against bacterial biofilms have been observed, likely due to disrupting bacterial chemical signaling and possibly altering the structure of the substrate itself.

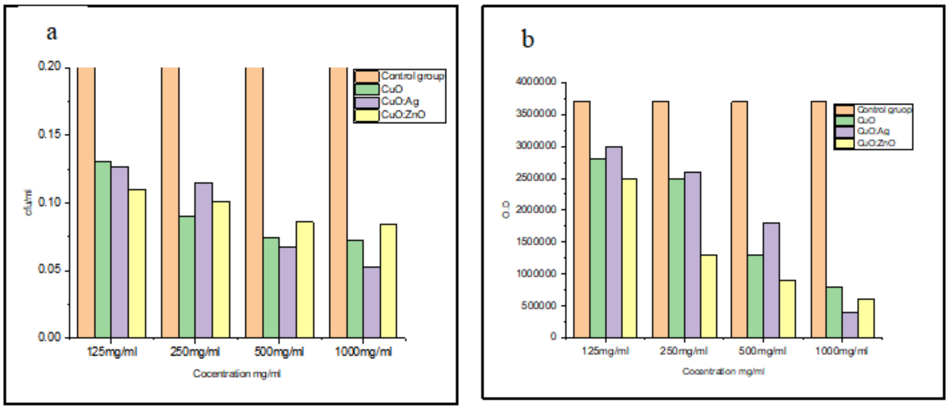


**Figure 7. The antibacterial efficacy of nanoparticles at different doses against Klebsiella pneumoniae (a) Bacteria adhesion (b) Biofilm formation**

## 4.CONCLUSIONS

Pure and Ag/Zn-doped CuO nanoparticles were produced by arc discharge at 5 A in deionized water, without electrolytes, reducing agents, or post-synthesis annealing. XRD confirmed the pure monoclinic phase of CuO, and Ag and ZnO phases were clearly detected in the doped samples.SEM images showed porous, aggregated nanostructures with increased surface roughness after doping. Ag and ZnO doping considerably improved methylene blue degradation, with CuO:Ag (>98%, 90 min) and CuO:ZnO (>95%, 60 min) outperforming pure CuO (~92–93%, 135 min). Against Klebsiella pneumoniae, CuO:Ag was most effective against bacterial adhesion, while CuO:ZnO showed the strongest biofilm activity. These results indicate that arc discharge in liquid is a simple, inexpensive, and an economical route for the growth of CuO nanoparticles for water therapy and antibacterial applications.

## 5.REFERENCES

[1] R.G. Chaudhuri, S. Paria, Core/shell nanoparticles: classes, properties, synthesis mechanisms, characterization, and applications, Chem. Rev. 112(4) (2011) 2373–2433.

[2] Q. Jiao, L. Li, Q. Mu, Q. Zhang, Immunomodulation of nanoparticles in nanomedicine applications, BioMed Res. Int. 2014 (2014) 1–19.

[3] N.K. Kaushik, N. Kaushik, N.N. Linh, B. Ghimire, A. Pengkit, J. Sornsakdanuphap, S.J. Lee, E.H. Choi, Plasma and nanomaterials: fabrication and biomedical applications, Nanomaterials 9(1) (2019) 98.

[4] K. Zhou, X. Zhou, J. Liu, Z. Huang, Application of magnetic nanoparticles in petroleum industry: a review, J. Petrol. Sci. Eng. 188 (2020) 106943.

[5] Y. Lee, B. Bora, S. Yap, C. Wong, Effect of ambient air pressure on synthesis of copper and copper oxide nanoparticles by wire explosion process, Curr. Appl. Phys. 12(1) (2012) 199–203.

[6] P. Mahajan, A. Singh, R. Datt, V. Gupta, S. Arya, Realization of inverted organic solar cells by using sol-gel synthesized ZnO/Y2O3 core/shell nanoparticles as electron transport layer, IEEE J. Photovolt. 10(6) (2020) 1744–1749.

[7] N. Verma, N. Kumar, Synthesis and biomedical applications of copper oxide nanoparticles: An expanding horizon, ACS Biomater. Sci. Eng. 5 (2019) 1170–1188.

[8] K.S. Siddiqi, A. Husen, Current status of plant metabolite-based fabrication of copper/copper oxide nanoparticles and their applications: A review, Biomater. Res. 24 (2020) 11.

[9] H.M. Fahmy, N.M. Ebrahim, M.H. Gaber, In-vitro evaluation of copper/copper oxide nanoparticles cytotoxicity and genotoxicity in normal and cancer lung cell lines, J. Trace Elem. Med. Biol. 60 (2020) 126481.

[10] D.A. Rippner, A.J. Margenot, S.C. Fakra, Microbial response to copper oxide nanoparticles in soils is controlled by land use rather than copper fate, Environ. Sci. Nano 8 (2021) 3560–3576.

[11] E. Abou-Salem, A.R. Ahmed, M. Elbagory, A.E. Omara, Efficacy of biological copper oxide nanoparticles on controlling damping-off disease and growth dynamics of sugar beet (Beta vulgaris L.) plants, Sustainability 14 (2022) 12871.

[12] A.J. Margenot, D.A. Rippner, M.R. Dumlao, S. Nezami, Copper oxide nanoparticle effects on root growth and hydraulic conductivity of two vegetable crops, Plant Soil 431 (2018) 333–345.
[13] A.S. Zoolfakar, R.A. Rani, A.J. Morfa, Nanostructured copper oxide semiconductors: A perspective on materials, synthesis methods and applications, J. Mater. Chem. C 27 (2014) 5247–5270.
[14] S. Saleem, A.H. Jabbar, M.H. Jameel, Enhancement in structural, morphological, and optical properties of copper oxide for optoelectronic device applications, Nanotechnol. Rev. 11 (2022) 2827–2838.
[15] G. Bhanjana, N. Dilbaghi, K. Kim, Low temperature synthesis of copper oxide nanoflowers for lead removal using sonochemical route, J. Mol. Liq. 244 (2017) 506–511.
[16] M.A. Khan, N. Nayan, M.K. Ahmad, Advanced nanoscale surface characterization of CuO nanoflowers for significant enhancement of catalytic properties, Molecules 26 (2021) 2700.
[17] C. Chimeno-Trinchet, A. Fernandez-Gonzalez, J.A.G. Calzon, Alkyl-capped copper oxide nanospheres and nanoprolates for sustainability: Water treatment and improved lubricating performance, Sci. Technol. Adv. Mater. 20 (2019) 657–672.
[18] S. Kumar, A.K. Ojha, D. Bhorolua, Facile synthesis of CuO nanowires and Cu2O nanospheres grown on rGO surface and exploiting its photocatalytic, antibacterial and supercapacitive properties, Physica B 558 (2019) 74–81.
[19] J. Zhang, J. Liu, Q. Peng, Nearly monodisperse Cu2O and CuO nanospheres: Preparation and applications for sensitive gas sensors, Chem. Mater. 18 (2006) 867–871.
[20] S. Steinhauer, Gas sensors based on copper oxide nanomaterials: A review, Chemosensors 9 (2021) 51.
[21] K.P. Jithul, K.S. Samra, Cupric oxide based supercapacitors: A review, J. Phys. Conf. Ser. 2267 (2022) 012120.
[22] K. Midander, P. Cronholm, H.L. Karlsson, Surface characteristics, copper release, and toxicity of nano- and micrometer-sized copper and copper(II) oxide particles: A cross-disciplinary study, Small 5 (2009) 389–399.
[23] U.T. Khatoon, A. Velidandi, G.V.S. Nageswara Rao, Copper oxide nanoparticles: Synthesis via chemical reduction, characterization, antibacterial activity, and possible mechanism involved, Inorg. Chem. Commun. 149 (2023) 110372.
[24] S. Chen, A. Zehri, Q. Wang, Manufacturing graphene-encapsulated copper particles by chemical vapor deposition in a cold wall reactor, ChemistryOpen 8 (2019) 58–63.
[25] R. Rawat, A. Tiwari, N. Arun, Synthesis of CuO hollow nanoparticles using laser ablation: Effect of fluence and solvents, Appl. Phys. A 126 (2020) 226.
[26] M. Patel, S. Mishra, R. Verma, Synthesis of ZnO and CuO nanoparticles via sol–gel method and its characterization by using various techniques, Discov. Mater. 2 (2022) 1.
[27] Z. Alhalili, Green synthesis of copper oxide nanoparticles (CuO NPs) from Eucalyptus globulus leaf extract: Adsorption and design of experiments, Arab. J. Chem. 15 (2022) 103739.
[28] N. Zulfiqar, F. Inam, I. Khudayberganov, S. Kurbanova, Sustainable synthesis and photocatalytic insights into Ag-doped copper oxide nanoparticles: a comparative study, Sci. Rep. (2026).
[29] A.N. Kumar, M. Balakrishna, U. Desai, R. Rakshith, K.M. Ambika, P. Soumya, et al., Solution combustion synthesis of ZnO doped CuO nanocomposite for photocatalytic and sensor applications, Sci. Rep. 15(1) (2025) 338.
[30] A.A. Efimov, D.V. Kornyushin, A.I. Buchnev, E.I. Kameneva, A.A. Lizunova, Fabrication of conductive and gas-sensing microstructures using focused deposition of copper nanoparticles synthesized by spark discharge, Appl. Sci. 11 (2021) 5791.
[31] X. Glad, J. Profili, M.S. Cha, A. Hamdan, Synthesis of copper and copper oxide nanomaterials by electrical discharges in water with various electrical conductivities, J. Appl. Phys. 127(2) (2020).
[32] P. Pootawang, N. Saito, S.Y. Lee, Discharge time dependence of a solution plasma process for colloidal copper nanoparticle synthesis and particle characteristics, Nanotechnology 24(5) (2013) 055604.
[33] M.V. Fomina, I.V. Gladysheva, O.V. Bakina, S.V. Cherkasov, I.F. Karimov, The bioactivity of Janus-like CuO–Ag nanoparticles on antibiotic-resistant clinical isolates of Klebsiella pneumoniae and their mechanism of action, Curr. Microbiol. 82(9) (2025) 433.
[34] Oneizah, L. H. A., Kareem, Q. S., & Shaheed, M. A. (2025, March). Investigation of the non-linear optical characteristics of gold nanoparticles doped with distilled water (DDDW) by laser. In AIP Conference Proceedings (Vol. 3264, No. 1, p. 040022). AIP Publishing LLC..
[35] S.Y. Xie, Z.J. Ma, C.F. Wang, Preparation and self-assembly of copper nanoparticles via discharge of copper rod electrodes in a surfactant solution: A combination of physical and chemical processes, J. Solid State Chem. 177 (2004) 3743–3747.
[36] Y.S. Park, S. Kodama, H. Sekiguchi, Preparation of metal nitride particles using arc discharge in liquid nitrogen, Nanomaterials 11 (2021) 2214.
[37] A.V. Ushakov, I.V. Karpov, A.A. Lepeshev, Influence of the oxygen concentration on the formation of crystalline phases of ZrO2 nanoparticles during the low-pressure arc-discharge plasma synthesis, Phys. Solid State 57 (2015) 2320–2322.
[38] R. Burlica, K.Y. Shih, B.R. Locke, Formation of H2 and H2O2 in a water-spray gliding arc nonthermal plasma reactor, Ind. Eng. Chem. Res. 49 (2010) 6342–6349.
[39] A.M. El-Khatib, M.S. Badawi, Z.F. Ghatass, Synthesize of silver nanoparticles by arc discharge method using two different rotational electrode shapes, J. Clust. Sci. 29 (2018) 1169–1175.
[40] V. Lakshmi Prasanna, R. Vijayaraghavan, Insight into the mechanism of antibacterial activity of ZnO: surface defects mediated reactive oxygen species even in the dark, Langmuir 31(33) (2015) 9155–9162.
[41] Sami, W. A., Khadayier, A. A., & Shaheed, M. A. (2026). Synthesis and PVP Coating Effects on Cadmium Ferrites for Antibacterial Applications. Iraqi Journal of Science, 1580-1587.
[42] X. Yang, et al., Modified Titanium dioxide-based photocatalysts for water treatment: Mini review, Environ. Funct. Mater. 3(1) (2024) 1–12.

[40] C. Lin, J. Liao, Production of CuO nanoparticles using a simple precipitation method in a rotating packed bed with blade packings, J. Alloys Compd. 775 (2018) 419–426.
[41] H.T. Assaouka, D.M. Daawe, R.L. Fomekong, I.N. Nsangou, P.M. Kouotou, Inexpensive and easily replicable precipitation of CuO nanoparticles for low temperature carbon monoxide and toluene catalytic oxidation, Heliyon 8(9) (2022).
[42] D. Renuga, J. Jeyasundari, A.S. Shakthi Athithan, Y. Brightson Arul Jacob, Synthesis and characterization of copper oxide nanoparticles using Brassica oleracea var. italic extract for its antifungal application, Mater. Res. Express 7(4) (2020) 045007.
[43] T.A.T. Sallehudin, M.N.A. Seman, S.M.S.T. Chik, Preparation and characterization silver nanoparticle embedded polyamide nanofiltration (NF) membrane, MATEC Web Conf. 150 (2018) 02003.
[44] A.M. Raba-Páez, J.O.D. Malafatti, C.A. Parra-Vargas, E.C. Paris, M. Rincón-Joya, Effect of tungsten doping on the structural, morphological and bactericidal properties of nanostructured CuO, PLoS One 15(9) (2020) e0239868.
[45] E. Saebnoori, N. Koupaei, S.A. Hassanzadeh Tabrizi, The solution plasma synthesis, characterisation, and antibacterial activities of dispersed CuO nanoparticles, Mater. Technol. 37(9) (2022) 1220–1229.
[46] M. Farooq, S. Shujah, K. Tahir, S.T. Hussain, A.U. Khan, Z.M. Almarhoon, et al., Phytoassisted synthesis of CuO and Ag–CuO nanocomposite, characterization, chemical sensing of ammonia, degradation of methylene blue, Sci. Rep. 14(1) (2024) 1618.
[47] B. Li, Y. Li, Y. Zhao, L. Sun, Shape-controlled synthesis of Cu2O nano/microcrystals and their antibacterial activity, J. Phys. Chem. Solids 74(12) (2013) 1842–1847.
[48] L. Dong, S. Chen, Z. Zhao, X. Sun, G. Lv, W. Wang, et al., Template-Directed Growth of a 3D Hierarchical Structure of Well-Aligned Bimetallic MOF Arrays for High-Efficiency Electrocatalytic Air Sterilization, Engineering (2025).
[49] A.S. Zhakypov, R.R. Nemkayeva, Y. Yerlanuly, M.A. Tulegenova, B.Y. Kurbanov, M.B. Aitzhanov, et al., Synthesis and in situ oxidation of copper micro- and nanoparticles by arc discharge plasma in liquid, Sci. Rep. 13(1) (2023) 15714.
[50] S.O. Mohammed, M.M. Khalil, I.M. El-Sewify, A. Radwan, Nd-doped CuO/ZnO and ZnO/CuO heterojunctions for simultaneous UV blocking and malachite green detoxification, Sci. Rep. 15(1) (2025) 34063.
[51] T. Nittaya, L. Chaikarn, P. Sukon, Synthesis of thermally spherical CuO nanoparticles, J. Nanomater. 2014 (2014) 1–5.
[52] R.S. Mohammed, K.A. Aadim, K.A. Ahmed, Synthesis of CuO/ZnO and MgO/ZnO core/shell nanoparticles with plasma jets and study of their structural and optical properties, Karbala Int. J. Mod. Sci. 8(2) (2022) 88–97.
[53] A.I. Khedr, M.H. Ali, Eco-friendly fabrication of copper oxide nanoparticles using peel extract of Citrus aurantium for the efficient degradation of methylene blue dye, Sci. Rep. 14(1) (2024) 29156.
[54] P. Shanmugam, R.C. Ngullie, S.M. Smith, S. Boonyuen, R. Boddula, R. Pothu, Visible-light induced photocatalytic removal of methylene blue dye by copper oxide decorated zinc oxide nanorods, Mater. Sci. Energy Technol. 6 (2023) 359–367.
[55] H. Algadi, M.A. Alhoot, L.A. Yaaqoob, Copper Oxide Nanoparticles: Antibacterial Efficacy and Biofilm Inhibition in Klebsiella pneumoniae, J. Pure Appl. Microbiol. 19(4) (2025).
[56] M.V. Fomina, I.V. Gladysheva, O.V. Bakina, S.V. Cherkasov, I.F. Karimov, The Bioactivity of Janus-like CuO–Ag Nanoparticles on Antibiotic-Resistant Clinical Isolates of Klebsiella pneumoniae and their Mechanism of Action, Curr. Microbiol. 82(9) (2025) 433.
[57] M. Jayanetti, C. Thambiliyagodage, H. Liyanaarachchi, G. Ekanayake, A. Mendis, L. Usgodaarachchi, In vitro influence of PEG functionalized ZnO–CuO nanocomposites on bacterial growth, Sci. Rep. 14(1) (2024) 1293.
[58] A.K. El-Sawaf, S.H. El-Moslamy, E.A. Kamoun, K. Hossain, Green synthesis of trimetallic CuO/Ag/ZnO nanocomposite using Ziziphus spina-christi plant extract: characterization, statistically experimental designs, and antimicrobial assessment, Sci. Rep. 14(1) (2024) 19718.
[59] A.M. Shehabeldine, B.H. Amin, F.A. Hagras, A.A. Ramadan, M.R. Kamel, M.A. Ahmed, et al., Potential antimicrobial and antibiofilm properties of copper oxide nanoparticles: time-kill kinetic essay and ultrastructure of pathogenic bacterial cells, Appl. Biochem. Biotechnol. 195(1) (2023) 467–485.
[60] M. Ghosh, D. Ghosh, S. Paul, D. Datta, S.K. Mukhopadhyay, S.K. Pradhan, Development of a biocompatible CuO-ZnO nanocomposite for targeting of Chloramphenicol with enhanced antibacterial and anti-biofilm efficacy, J. Pharm. Sci. (2025) 104080.
[61] T. Saklani, N.C. Joshi, V. Jakhmola, Biofabrication, Characterisation and Antimicrobial Activity of CuO/Ag-based Material, J. Pure Appl. Microbiol. 18(2) (2024).
[62] F. Alhosani, D. Islayem, S. Almansoori, A. Zaka, L. Nayfeh, A. Rezk, et al., Antibiofilm activity of ZnO–Ag nanoparticles against Pseudomonas aeruginosa, Sci. Rep. 15(1) (2025) 17321.